

## **Evaluation of Bacterial RNA Polymerase Inhibitors in a *Staphylococcus aureus*-Based Wound Infection Model in SKH1 Mice**

Jörg Haupenthal<sup>1,\*</sup>, Yannik Kautz<sup>2</sup>, Walid A. M. Elgaher<sup>1</sup>, Linda Pätzold<sup>2</sup>, Teresa Röhrig<sup>1</sup>, Matthias W. Laschke<sup>3</sup>, Thomas Tschernig<sup>4</sup>, Anna K. H. Hirsch<sup>1,5</sup>, Vadim Molodtsov<sup>6,7</sup>, Katsuhiko S. Murakami<sup>6</sup>, Rolf W. Hartmann<sup>1,5</sup> and Markus Bischoff<sup>2</sup>

<sup>1</sup> Department of Drug Design and Optimization, Helmholtz Institute for Pharmaceutical Research Saarland (HIPS) – Helmholtz Centre for Infection Research (HZI), Campus Building E8.1, 66123 Saarbrücken, Germany

<sup>2</sup> Institute of Medical Microbiology and Hygiene, Saarland University, 66421 Homburg/Saar, Germany

<sup>3</sup> Institute for Clinical & Experimental Surgery, Saarland University, 66421 Homburg/Saar, Germany

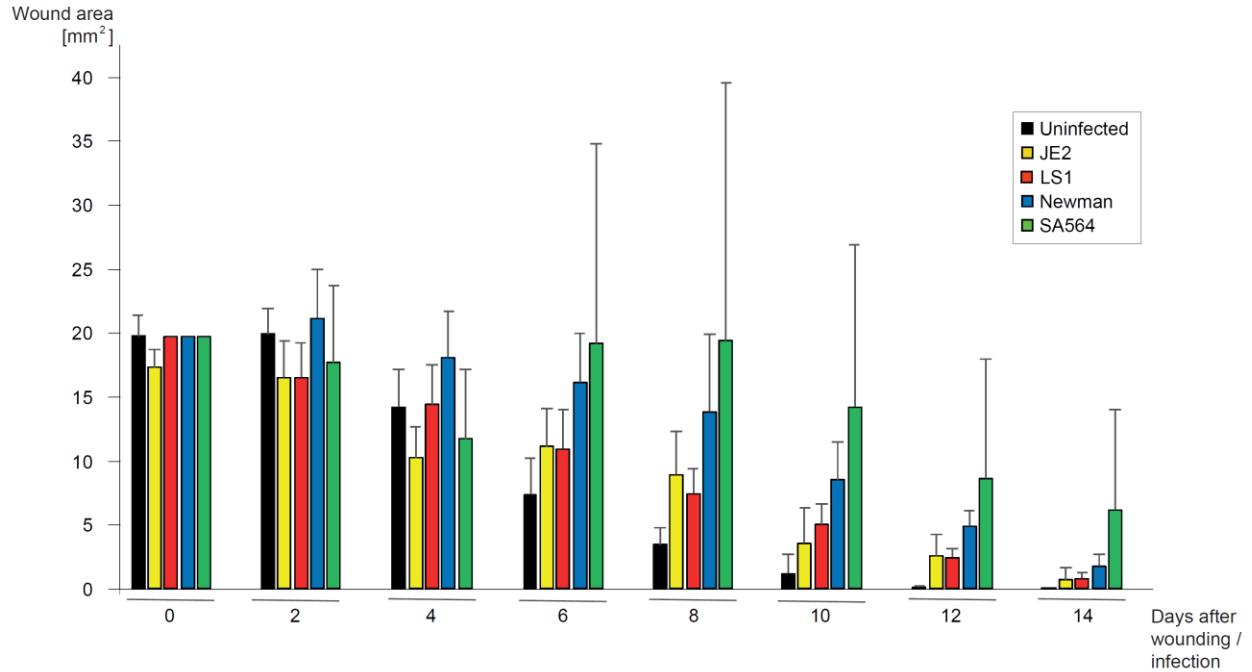
<sup>4</sup> Institute of Anatomy and Cell Biology, Saarland University, 66421 Homburg/Saar, Germany

<sup>5</sup> Department of Pharmacy, Saarland University, Campus Building E8.1, 66123 Saarbrücken, Germany

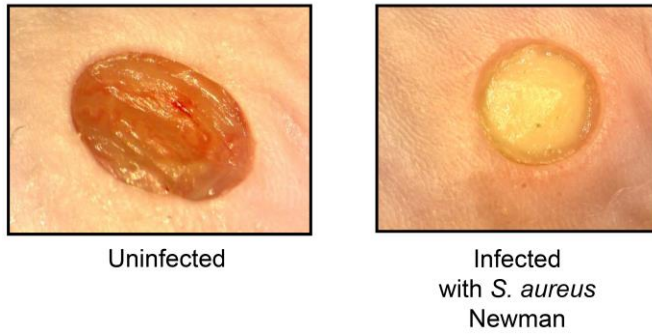
<sup>6</sup> Department of Biochemistry and Molecular Biology, The Center for RNA Molecular Biology, The Pennsylvania State University, University Park, PA 16802, USA

<sup>7</sup> Current address: Waksman Institute and Department of Chemistry, Rutgers University, Piscataway NJ 08854, USA

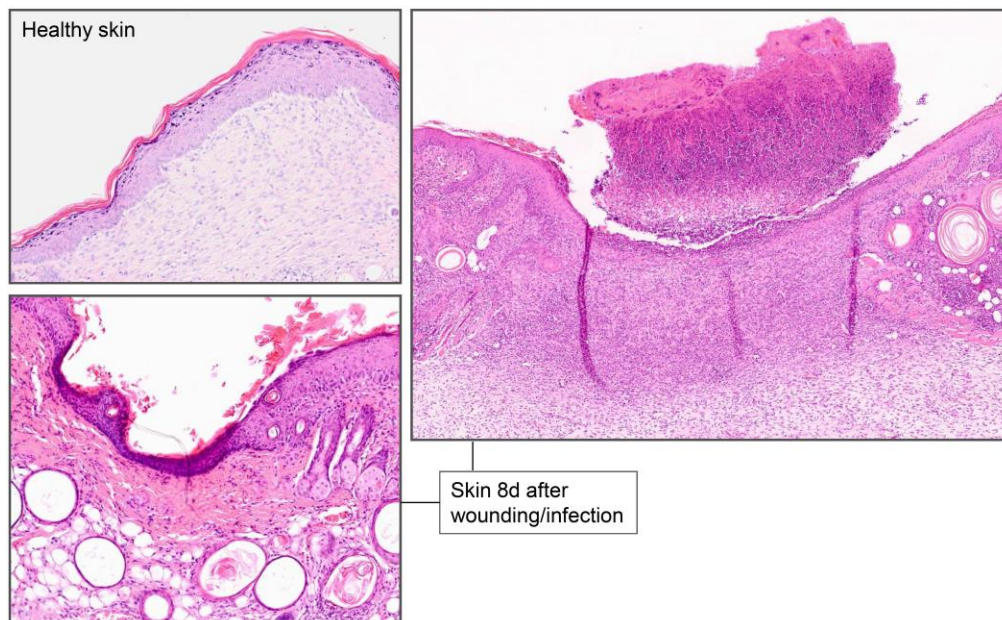
\* Corresponding author. E-mail: Joerg.Haupenthal@Helmholtz-HIPS.de



**Figure S1: Influence of different *S. aureus* strains on wound healing.** SKH1 mice were wounded twice dorsally with a 5 mm (diameter) biopsy punch and subsequently infected with 10  $\mu$ L (OD 1.0) of either the *S. aureus* strain JE2, LS1, Newman or SA564. On day 0 and then every two days until day 14, the wound sizes were determined and compared to uninfected wounds. At least eight wounds per group were examined. Based on the wound sizes measured and the standard deviations in these experiments we chose to perform the following experiments with the *S. aureus* Newman strain.

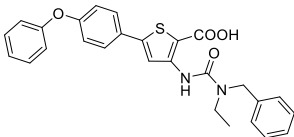
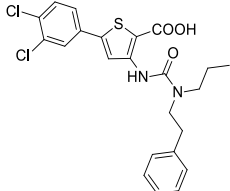
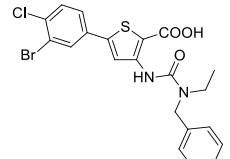
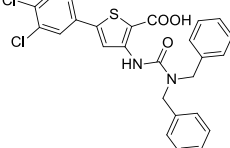
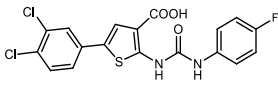
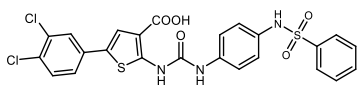


**Figure S2:** Illustration of an uninfected punch wound (left image) and a punch wound infected with *S. aureus* Newman (right image). Pictures were taken 48 h after punch wound formation and (non-)infection.



**Figure S3:** Haematoxylin and eosin (H&E) staining of paraffin sections. Healthy (upper left) and wounded and infected (with *S. aureus* Newman) skin sections (lower left and right, respectively) are shown eight days after wounding/infection.

**Table S1: Biological evaluation of selected RNAP inhibitors.** Our six most promising compounds with ureidothiophene-2/3-carboxylic acid core structure showed RNAP inhibition with IC<sub>50</sub> values in the one to two digit μM range, as published previously<sup>1-3</sup>. This inhibition was accompanied by a high antibacterial potency against *S. aureus* Newman, a sufficient solubility in PBS (1% DMSO) and a moderate to low cytotoxicity.

Compound	MIC SA-N (μg/mL)	RNAP inhibition (IC <sub>50</sub> in μM)	Cytotoxicity in HEK293 / NHDF cells (IC <sub>50</sub> in μM)	Solubility in PBS (μM)
<p><b>1</b></p> 	4	14	61 / >100	100
<p><b>2</b></p> 	2	12	64 / >100	40
<p><b>3</b></p> 	4	16	65 / >100	100
<p><b>4</b></p> 	3	6	53 / >100	40
<p><b>5</b></p> 	4	14	68 / >100	100
<p><b>6</b></p> 	3	8	91 / >100	20

**Table S2: Data collection and refinement statistics of the RNAP–compound 1 complex.** Data sets were collected at MacCHESS F1 line, Ithaca, NY. \*Highest resolution shells are shown in parentheses.

PDB ID	6VJS
<b>Data collection</b>	
Space group	P2 <sub>1</sub> 2 <sub>1</sub> 2 <sub>1</sub>
Cell dimensions	
<i>a</i> (Å)	187.077
<i>b</i> (Å)	205.501
<i>c</i> (Å)	309.88
Resolution (Å)	50 – 4.0
Total reflections	553,863
Unique reflections	99,376
Redundancy	5.6 (5.2)
Completeness (%)	99.44 (96.49)
<i>I</i> / $\sigma$	11.02 (1.95)
Wilson B-factor	157.43
R-merge	0.1056 (0.8696)
R-meas	0.1167 (0.9644)
CC <sup>1/2</sup>	0.998 (0.728)
CC*	0.999 (0.918)
<b>Refinement</b>	
Resolution (Å)	50 – 4.0
Reflections used in refinement	99,302 (9,503)
<i>R</i> <sub>work</sub>	0.2080 (0.2902)
<i>R</i> <sub>free</sub>	0.2667 (0.3644)
CC(work)	0.953 (0.798)
CC(free)	0.936 (0.631)
No. of atoms	56,011
macromolecules	55,971
ligands	34
R.m.s deviations	
bond length (Å)	0.003
bond angles (°)	0.84
Clashscore	15.2
Ramachandran favored (%)	85.82
Ramachandran outliers (%)	0.81
Average B-factor	206.74
macromolecules	206.79
ligands	136.90
Number of TLS groups	37

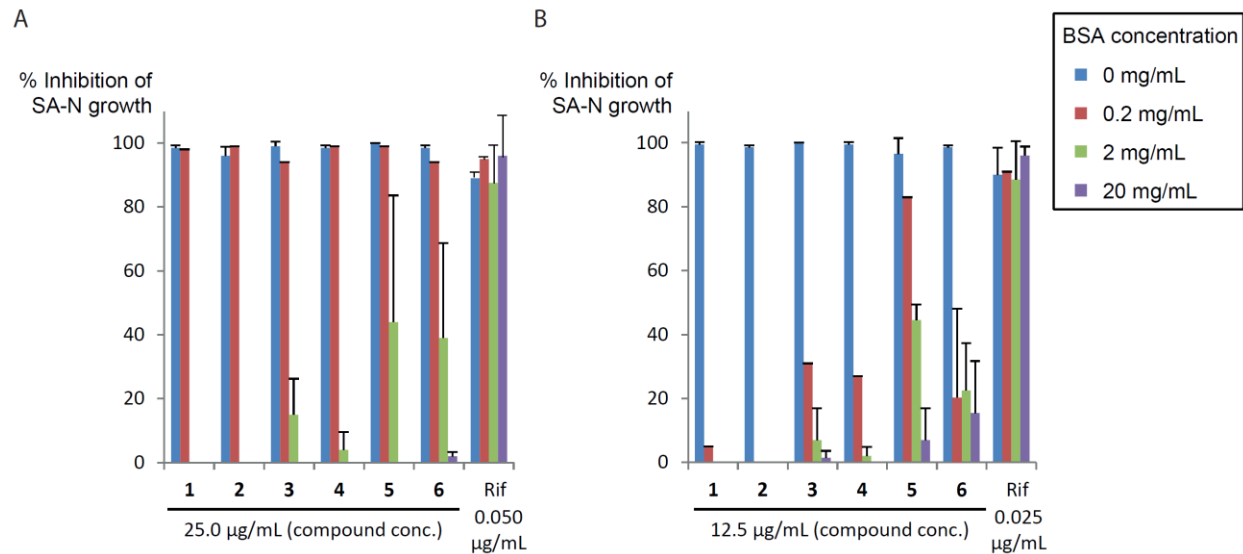


**Figure S4:** Concentration-dependent influence of bovine serum albumin (BSA) on the antibacterial activity of compounds 1–6 and rifampicin (Rif). Increasing concentrations of BSA (0 to 20 mg/mL) were incubated together with (A) 25 µg/mL of compounds 1–6 or 0.05 µg/mL of Rif and in parallel (B) together with 12.5 µg/mL of compounds 1–6 or 0.025 µg/mL of Rif.

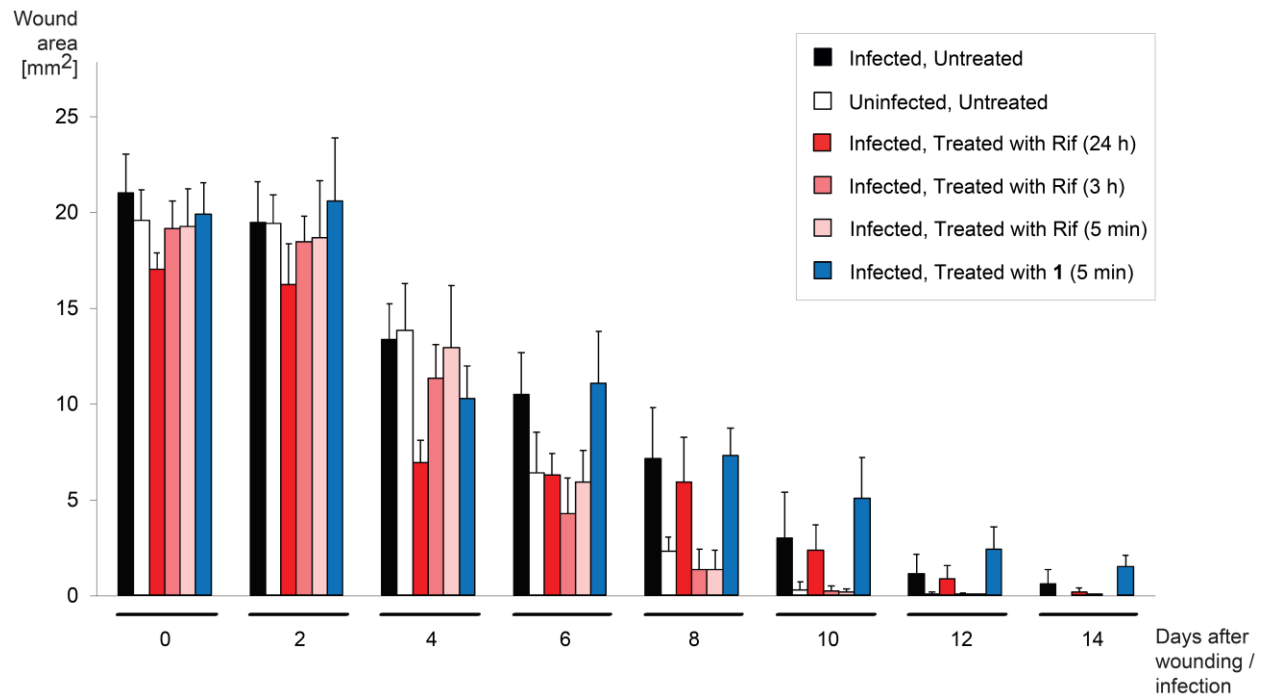


**Figure S5: Development of wound size.** The averaged wound areas (in mm<sup>2</sup>) are displayed every 2 d for the different treatment groups, between 0 and 14 d after wounding/infection.

**Table S3: Number of animals or wounds per experimental group.**

Referring to	Type of treatment	Animals or wounds	Number of animals/wounds
Figure 1	<i>S. aureus</i> OD 0.00	Animals	13
Figure 1	<i>S. aureus</i> OD 0.01	Animals	6
Figure 1	<i>S. aureus</i> OD 0.10	Animals	14
Figure 1	<i>S. aureus</i> OD 1.00	Animals	10
Figure S1	Uninfected	Wounds	16
Figure S1	<i>S. aureus</i> strain LS1	Wounds	8
Figure S1	<i>S. aureus</i> strain Newman	Wounds	8
Figure S1	<i>S. aureus</i> strain SA564	Wounds	8
Figure S1	<i>S. aureus</i> strain USA 300 JE2	Wounds	12
Figure 4	<i>S. aureus</i> OD 0.10 + PBS after 5 min and 48 h	Animals	14
Figure 4	PBS after 5 min and 48 h	Animals	8
Figure 4	<i>S. aureus</i> OD 0.10 + Rif after 24 h and 48 h	Animals	6
Figure 4	<i>S. aureus</i> OD 0.10 + Rif after 3 h and 48 h	Animals	5
Figure 4	<i>S. aureus</i> OD 0.10 + Rif after 5 min and 48 h	Animals	8
Figure 4	<i>S. aureus</i> OD 0.10 + Compound 1 after 5 min and 48 h	Animals	4
Figures 5 and S5	<i>S. aureus</i> OD 0.10 + PBS after 5 min and 48 h	Wounds	8
Figures 5 and S5	PBS after 5 min and 48 h	Wounds	10
Figures 5 and S5	<i>S. aureus</i> OD 0.10 + Rif after 24 h and 48 h	Wounds	12
Figures 5 and S5	<i>S. aureus</i> OD 0.10 + Rif after 3 h and 48 h	Wounds	10
Figures 5 and S5	<i>S. aureus</i> OD 0.10 + Rif after 5 min and 48 h	Wounds	8
Figures 5 and S5	<i>S. aureus</i> OD 0.10 + Compound 1 after 5 min and 48 h	Wounds	4
Figure 6	<i>S. aureus</i> OD 0.10 + PBS after 5 min and 48 h	Wounds	7
Figure 6	PBS after 5 min and 48 h	Wounds	14
Figure 6	<i>S. aureus</i> OD 0.10 + Rif after 24 h and 48 h	Wounds	12
Figure 6	<i>S. aureus</i> OD 0.10 + Rif after 3 h and 48 h	Wounds	10
Figure 6	<i>S. aureus</i> OD 0.10 + Rif after 5 min and 48 h	Wounds	8
Figure 6	<i>S. aureus</i> OD 0.10 + Compound 1 after 5 min and 48 h	Wounds	4



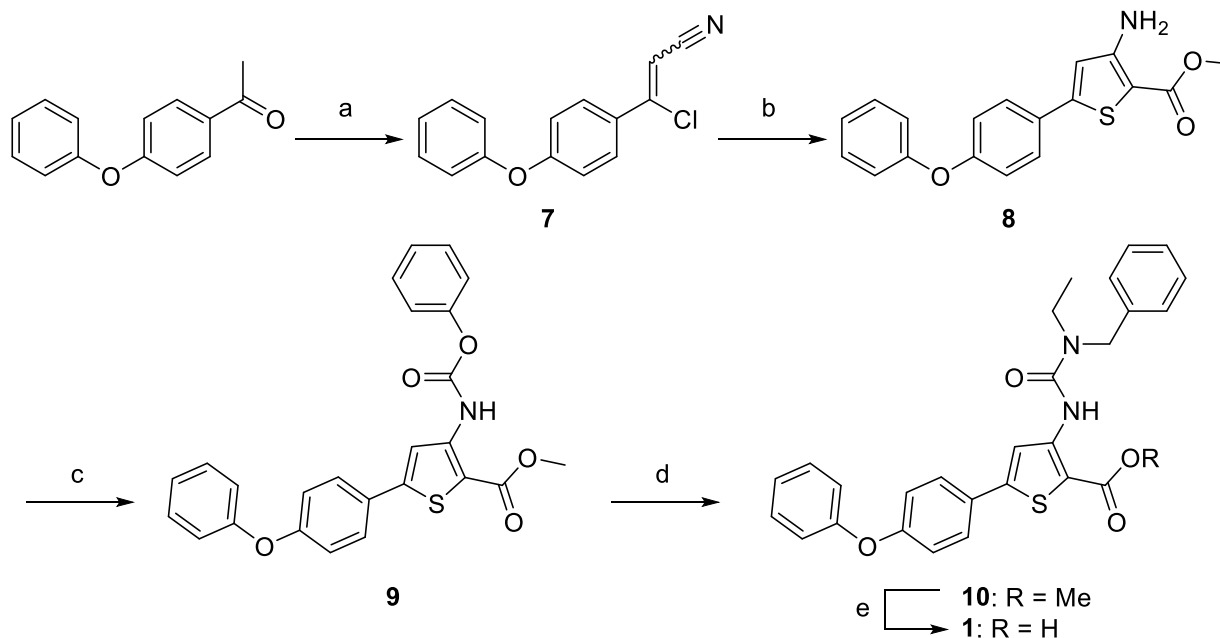
## **Materials and Methods**

### **Origin, synthesis and characterization of RNAP inhibitors**

Rifampicin was purchased from Merck (Darmstadt, Germany). Starting materials and solvents were purchased from commercial suppliers, and used without further purification. Reaction progress was monitored using TLC silica gel 60 F<sub>254</sub> aluminum sheets, and visualization was accomplished by UV at 254 nm. Flash chromatography was performed using silica gel 60 Å (40–63 µm). NMR spectra were recorded on a Bruker Avance Neo 500 MHz with CryoProbe Prodigy system (<sup>1</sup>H, 500 MHz; <sup>13</sup>C, 126 MHz) at 298 K. Chemical shifts were recorded as δ values in ppm units by reference to the hydrogenated residues of deuterated solvent as internal standard (CDCl<sub>3</sub>, δ = 7.27, 77.00; DMSO-d<sub>6</sub>, δ = 2.50, 39.51). Splitting patterns describe apparent multiplicities and are designated as s (singlet), br s (broad singlet), d (doublet), dd (doublet of doublet), t (triplet), q (quartet), m (multiplet). Coupling constants (*J*) are given in hertz (Hz). Weak or coalesced signals were elucidated by heteronuclear multiple quantum coherence (HMQC) and heteronuclear multiple bond coherence (HMBC) 2D-NMR techniques. Purity of all compounds used in biological assays was ≥ 95% as measured by Dionex UltiMate 3000 UHPLC<sup>+</sup> focused/Thermo Scientific Q Exactive Focus system (Thermo Fisher Scientific, Dreieich, Germany). The system consists of Dionex UltiMate 3000 pump, autosampler, column compartment, diode array detector, and single-quadrupole mass spectrometer, as well as the standard software Xcalibur for operation. RP EC 150/2 NUCLEODUR C18 Pyramid, 3 µm (150 mm × 2 mm) column (Macherey-Nagel, München, Germany) was used as stationary phase, and a binary solvent system A and B (A = water with 0.1% FA; B = MeCN with 0.1% FA) was used as mobile phase. In a gradient run, the percentage of B was increased from an initial concentration of 10% at 0 min to 95% at 5 min and kept at 95% for 1.2 min. The injection volume was 2 µL and flow rate was set to 500 µL/min. MS (ESI) analysis was carried out at a spray voltage of 3800 V, a capillary temperature of 350 °C, and a source CID of 55 V. Spectra were acquired in positive mode from 100 to 1400 m/z and at 254 nm for UV tracing. High-resolution mass spectrometry (HRMS) data was determined by a Thermo Scientific Q Exactive Focus system.

Synthesis and characterization of compounds **2–6** was described before<sup>1–3</sup>.

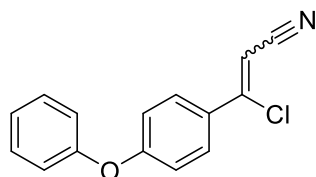
Synthesis of compound **1** started with chloroformylation of 4'-phenoxyacetophenone via Vilsmeier reagent (POCl<sub>3</sub>/DMF), followed by a dehydration with hydroxylamine hydrochloride to yield the β-chlorocinnamonitrile **7** according to a modified Vilsmeier–Haack–Arnold reaction (Scheme S1). Cyclization of **7** with methyl thioglycolate under reflux and basic conditions provided the 3-aminothiophene-2-carboxylate **8**. In contrast to previous procedures,<sup>2</sup> the ureido functional group was prepared using mild reagents via a phenyl carbamate intermediate **9**.<sup>3</sup> Subsequent nucleophilic substitution with *N*-ethylbenzylamine in DMSO delivered the 3-ureidothiophene-2-carboxylate **10**. Saponification of the methyl ester **10** afforded the free acid **1** (Scheme S1).



**Scheme S1. Synthesis of the 3-ureidothiophene-2-carboxylic acid 1.<sup>a</sup>**

<sup>a</sup>Reagents and conditions: (a) 1) DMF, POCl<sub>3</sub>, 0 °C–rt, 2 h, 2) NH<sub>2</sub>OH·HCl, rt, 16 h, 79%; (b) Na, MeOH, HSCH<sub>2</sub>COOMe, 70 °C, 16 h, 66%; (c) ClCOOPh, DCM, pyridine, rt, 12 h, 96%; (d) EtBnNH, DMSO, rt, 2 h, 97%; (e) KOH, MeOH/THF/H<sub>2</sub>O, 40 °C, 16 h, 94%.

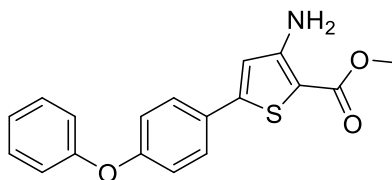
**3-Chloro-3-(4-phenoxyphenyl)acrylonitrile (7)**



To a stirred ice-cooled solution of 4'-phenoxyacetophenone (4.25 g, 20 mmol) in anhydrous DMF (40 mL, 0.51 mol, 25 equiv), POCl<sub>3</sub> (12.27 g, 80 mmol, 4 equiv) was added portionwise over 20 min keeping the temperature below 25 °C. The reaction was stirred at rt for 2 h, then hydroxylamine hydrochloride (1.53 g, 22 mmol, 1.1 equiv) was added cautiously (an exothermic reaction). The reaction was further stirred at rt for 16 h. Water (200 mL) was added and the mixture was extracted by EtOAc (3 × 150 mL). Organic layers were dried (MgSO<sub>4</sub>), filtered, and solvent was removed under reduced pressure. The crude material was sufficiently pure and was used directly for the next step without further purification.

Yield 79%; yellow liquid.

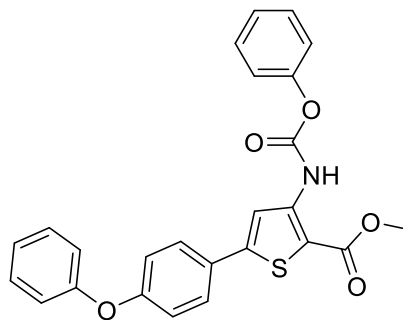
### Methyl 3-amino-5-(4-phenoxyphenyl)thiophene-2-carboxylate (**8**)



To a stirred ice-cooled anhydrous MeOH (50 mL) in a 100 mL two-neck round-bottom flask, sodium metal (483 mg, 21 mmol, 1.4 equiv) was added portionwise under nitrogen atmosphere. After complete dissolution of sodium, methyl thioglycolate (1.75 g, 16.5 mmol, 1.1 equiv) was added and the mixture was stirred at rt for 15 min.  $\beta$ -Chlorocinnamionitrile **7** (3.84, 15 mmol) was added and the reaction was stirred at 70 °C under reflux condition for 16 h. Solvent was removed under reduced pressure, water (100 mL) was added and the mixture was extracted by EtOAc (2 x 80 mL). Organic layers were dried (MgSO<sub>4</sub>), filtered, and solvent was removed under reduced pressure. The crude material was dissolved in toluene (3 mL) and was purified by flash chromatography (SiO<sub>2</sub>, petroleum ether 40/60–EtOAc = 6 : 1).

Yield 66%; yellowish white solid; <sup>1</sup>H NMR (500 MHz, CDCl<sub>3</sub>)  $\delta$  7.55 (d, *J* = 8.9 Hz, 2H), 7.38 (dd, *J* = 8.5, 7.5 Hz, 1H), 7.16 (tt, *J* = 7.5, 1.0 Hz, 1H), 7.06 (dd, *J* = 8.5, 1.0 Hz, 2H), 7.01 (d, *J* = 8.9 Hz, 2H), 6.71 (s, 1H), 5.49 (br s, 2H), 3.85 (s, 3H); <sup>13</sup>C NMR (126 MHz, CDCl<sub>3</sub>)  $\delta$  164.92, 158.28, 156.37, 154.36, 148.61, 129.89 (2C), 128.21, 127.41 (2C), 123.87, 119.39 (2C), 118.70 (2C), 114.94, 99.87, 51.27; HRMS (ESI+) calcd. for C<sub>18</sub>H<sub>16</sub>NO<sub>3</sub>S [M + H]<sup>+</sup>: 326.0851, found: 326.0838.

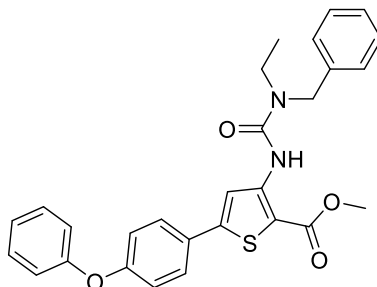
### Methyl 3-[(phenoxycarbonyl)amino]-5-(4-phenoxyphenyl)thiophene-2-carboxylate (**9**)



To a stirred ice-cooled solution of the 3-aminothiophene **8** (976 mg, 3 mmol) and pyridine (261 mg, 3.3 mmol, 1.1 equiv) in anhydrous DCM (20 mL), phenyl chloroformate (517 mg, 3.3 mmol, 1.1 equiv) was added dropwise. The reaction mixture was stirred at rt for 12 h. Solvent was removed under reduced pressure, and the residue was dissolved in EtOAc (50 mL). The organic layer was washed with 1 M HCl (2 x 25 mL), dried (MgSO<sub>4</sub>), filtered and solvent was removed under reduced pressure. The obtained material was sufficiently pure and was used directly for the next step without further purification.

Yield 96%; yellow liquid; HRMS (ESI+) calcd. for C<sub>25</sub>H<sub>20</sub>NO<sub>5</sub>S [M + H]<sup>+</sup>: 446.1062, found: 446.1049.

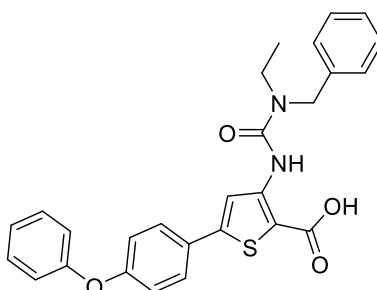
### Methyl 3-(3-benzyl-3-ethylureido)-5-(4-phenoxyphenyl)thiophene-2-carboxylate (**10**)



In a 50 mL two-neck round-bottom flask, the carbamate **9** (312 mg, 0.7 mmol) was dissolved in anhydrous DMSO (10 mL) under nitrogen atmosphere. *N*-Ethylbenzylamine (101 mg, 0.75 mmol, 1.07 equiv) was added dropwise and the reaction mixture was stirred at rt for 2 h. EtOAc (50 mL) was added and the organic layer was washed with 1 M HCl (2 × 30 mL), then 1 M NaOH (2 × 30 mL), dried (MgSO<sub>4</sub>), filtered and solvent was removed under reduced pressure. The obtained material was sufficiently pure and was used directly for the next step without further purification.

Yield 97%; yellow liquid; HRMS (ESI+) calcd. for C<sub>28</sub>H<sub>27</sub>N<sub>2</sub>O<sub>4</sub>S [M + H]<sup>+</sup>: 487.1692, found: 487.1684.

### 3-(3-Benzyl-3-ethylureido)-5-(4-phenoxyphenyl)thiophene-2-carboxylic acid (**1**)



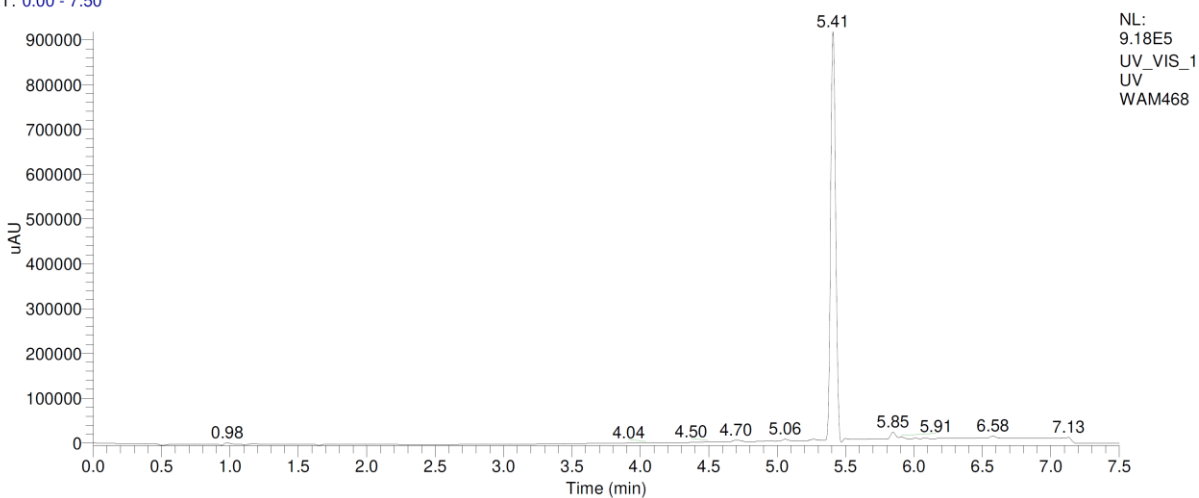
To a stirred solution of the thiophene-2-carboxylic acid methyl ester **10** (341 mg, 0.7 mmol) in MeOH–THF mixture (1:1, 20 mL), KOH (118 mg, 2.1 mmol, 3 equiv) in water (10 mL) was added. The reaction mixture was stirred at 40 °C for 16 h, then it was concentrated under reduced pressure. The residue was diluted with water (20 mL), cooled in an ice bath and acidified by KHSO<sub>4</sub> (saturated aqueous solution) to pH 4–5. The precipitated solid was extracted by EtOAc (2 × 30 mL). Organic layers were dried (MgSO<sub>4</sub>), filtered and solvent was removed under reduced pressure to afford the target compound **1**. The crude material was triturated with petroleum ether 40/60 (50 mL), stirred in a water bath at 40 °C for 10 min, cooled, and collected by filtration.

Yield 94%; off white solid; <sup>1</sup>H NMR (500 MHz, DMSO-*d*<sub>6</sub>) δ 13.37 (br s, 1H), 10.10 (br s, 1H), 8.23 (s, 1H), 7.72 (d, *J* = 8.7 Hz, 2H), 7.44 (t, *J* = 7.6 Hz, 2H), 7.35 (t, *J* = 7.0 Hz, 2H), 7.31 (d, *J* = 7.0 Hz, 2H), 7.27 (t, *J* = 7.0 Hz, 1H), 7.20 (t, *J* = 7.6 Hz, 1H), 7.10 (d, *J* = 7.6 Hz, 2H), 7.05 (d, *J* = 8.7 Hz, 2H), 4.58 (s, 2H), 3.38 (q, *J* = 7.0 Hz, 2H), 1.15 (t, *J* = 7.0 Hz, 3H); <sup>13</sup>C NMR (126 MHz, DMSO-*d*<sub>6</sub>) δ 165.83, 158.00, 155.79, 153.08, 147.26, 146.95, 138.17, 130.29 (2C), 128.56 (2C), 127.71, 127.66 (2C), 127.19 (3C), 124.25, 119.47 (2C), 118.74 (2C), 116.82, 106.27, 49.33, 41.83, 13.19; HRMS (ESI+) calcd. for C<sub>27</sub>H<sub>25</sub>N<sub>2</sub>O<sub>4</sub>S [M + H]<sup>+</sup>: 473.1535, found: 473.1522.

# UHPLC-HRMS, <sup>1</sup>H- and <sup>13</sup>C-NMR Spectra of the Described Compounds

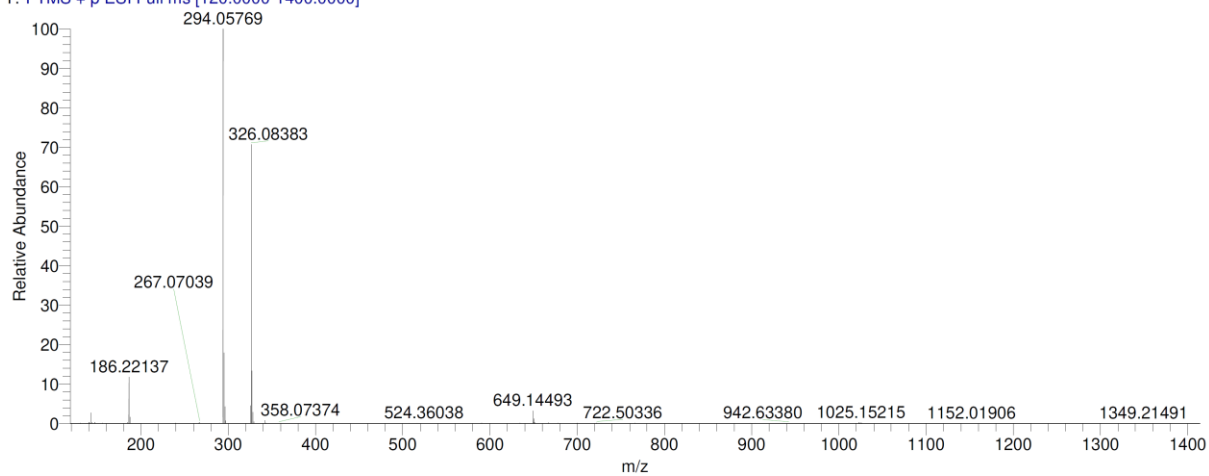
## Compound 8

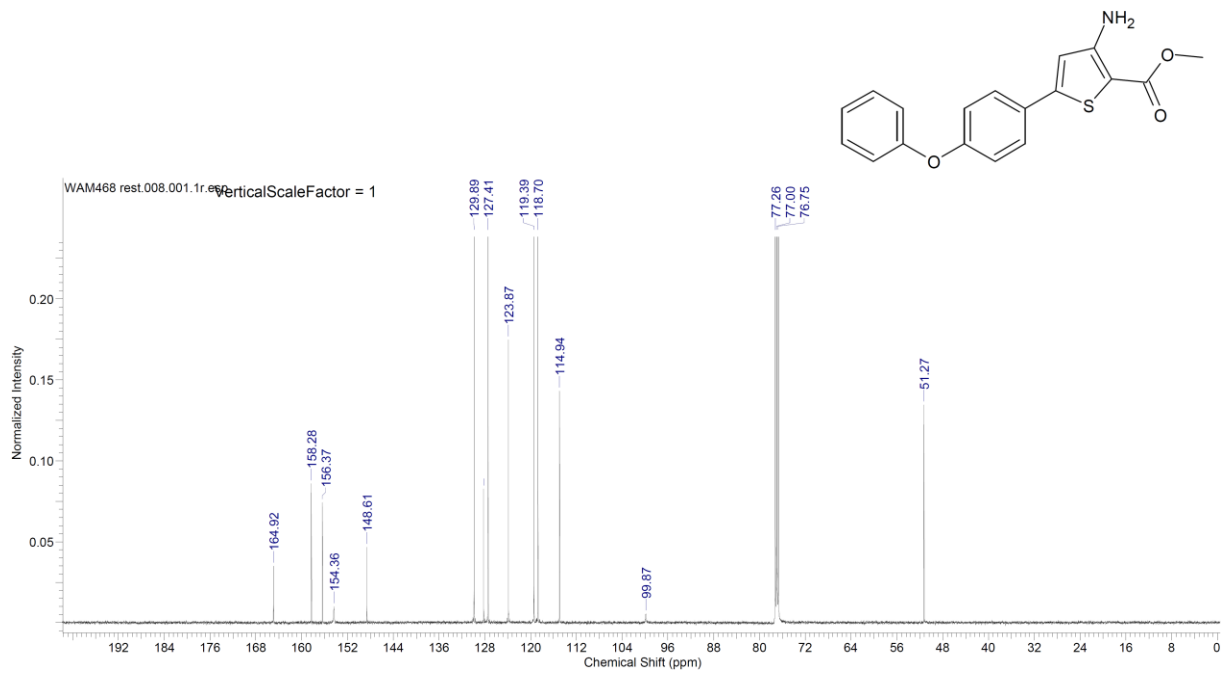
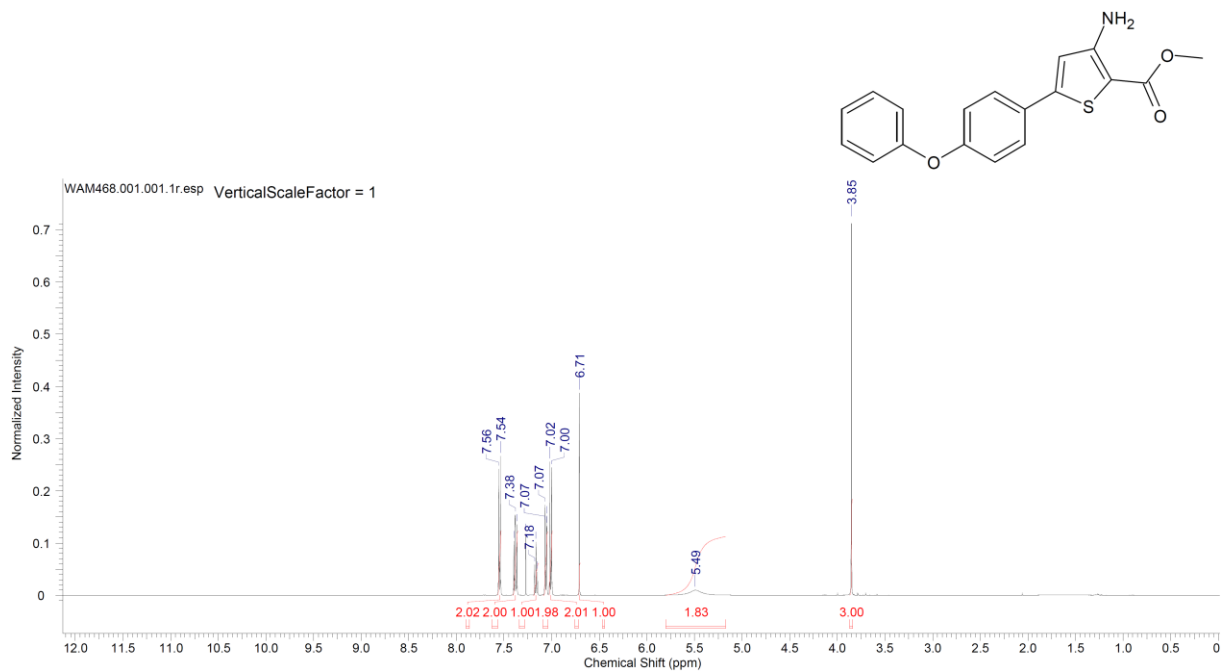
RT: 0.00 - 7.50



NL:  
9.18E5  
UV\_VIS\_1  
UV  
WAM468

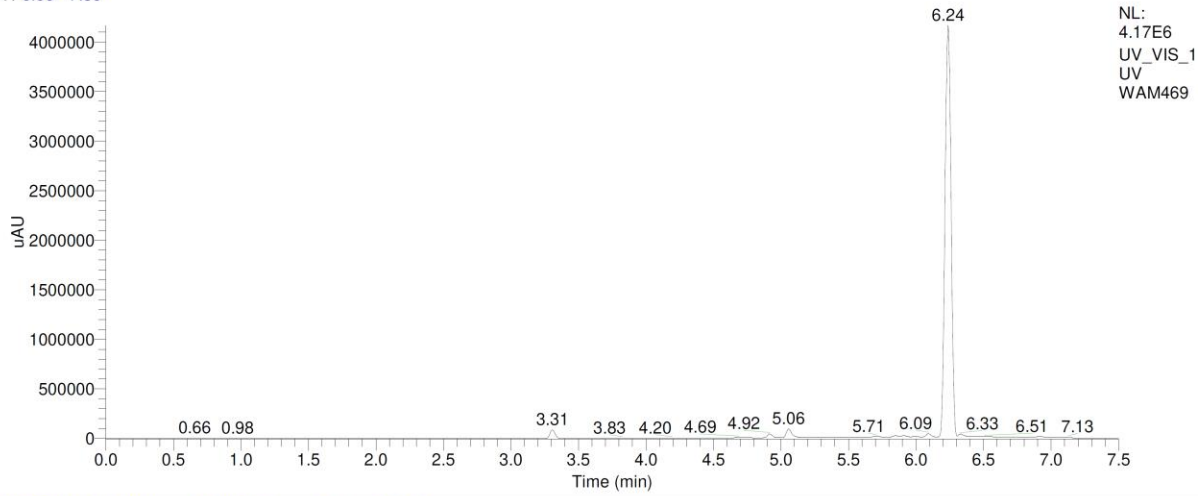
WAM468 #1207-1212 RT: 5.40-5.42 AV: 6 NL: 4.44E9  
T: FTMS + p ESI Full ms [120.0000-1400.0000]



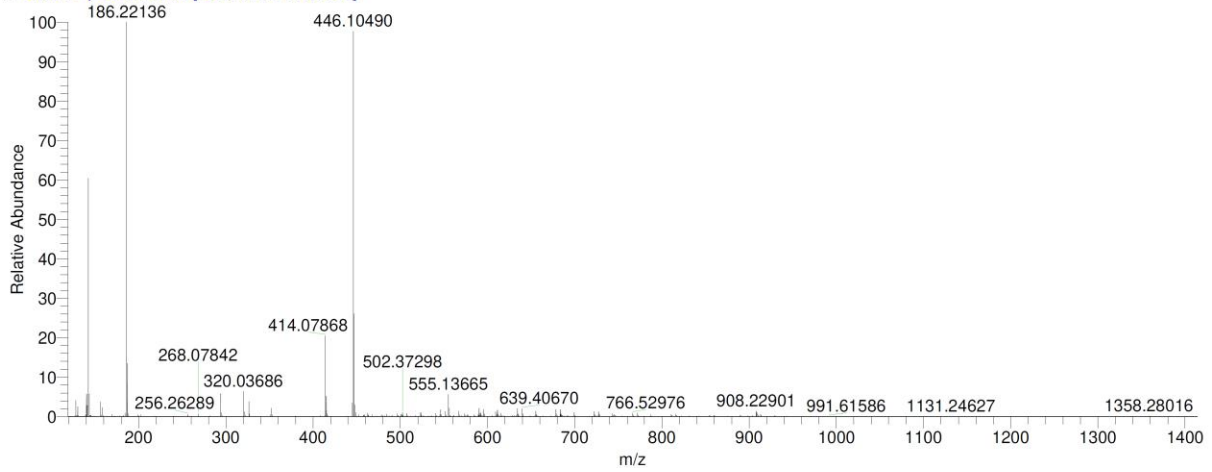


# Compound 9

RT: 0.00 - 7.50

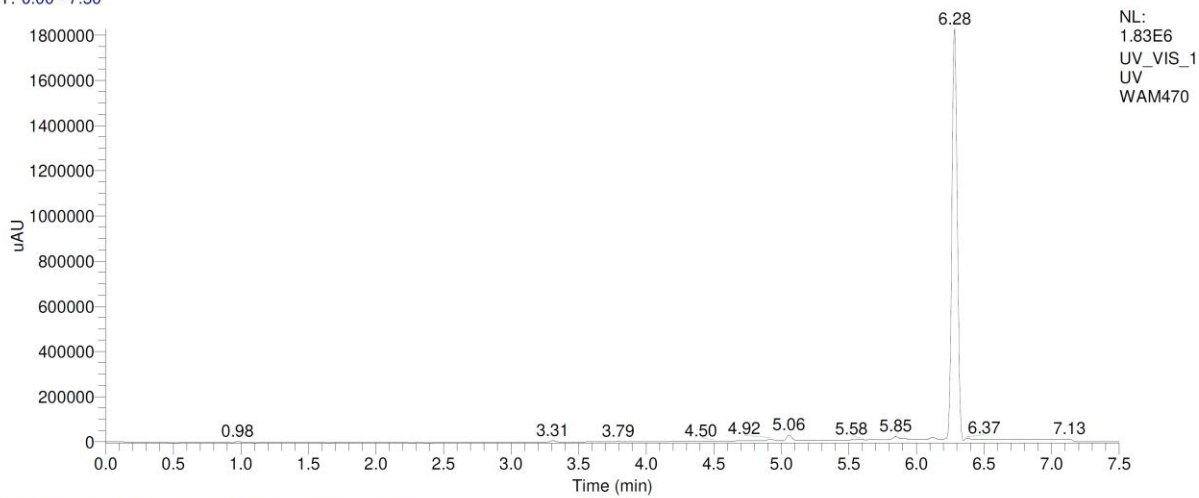


WAM469 #1394-1399 RT: 6.24-6.26 AV: 6 NL: 3.58E7  
T: FTMS + p ESI Full ms [120.0000-1400.0000]

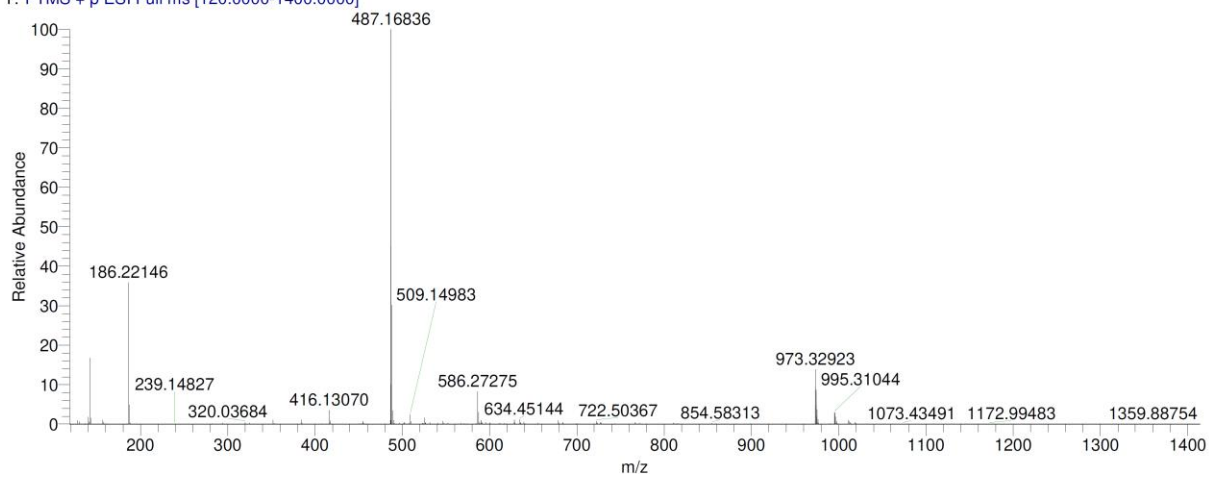


# Compound 10

RT: 0.00 - 7.50



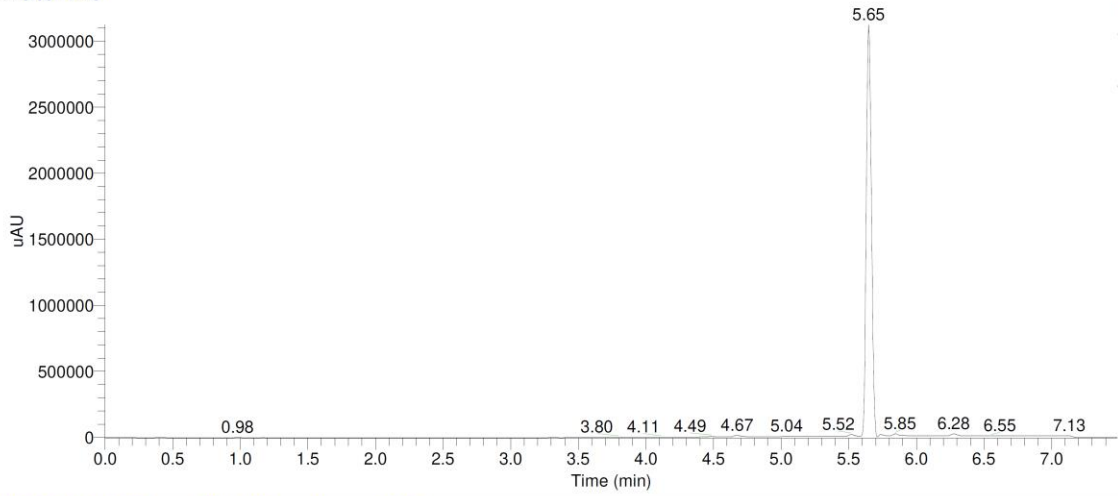
WAM470 #1401-1408 RT: 6.27-6.30 AV: 8 NL: 3.09E8  
T: FTMS + p ESI Full ms [120.0000-1400.0000]





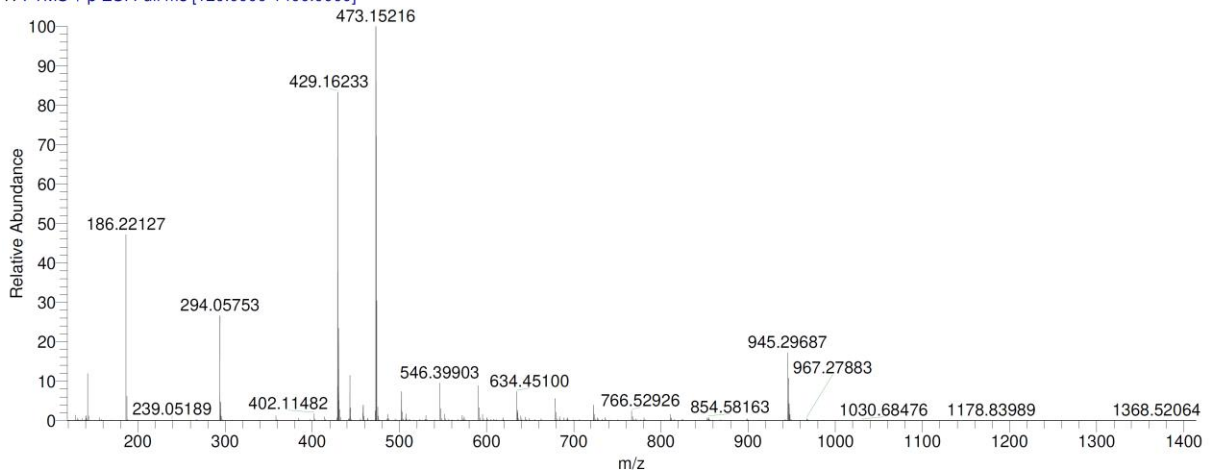
# Compound 1

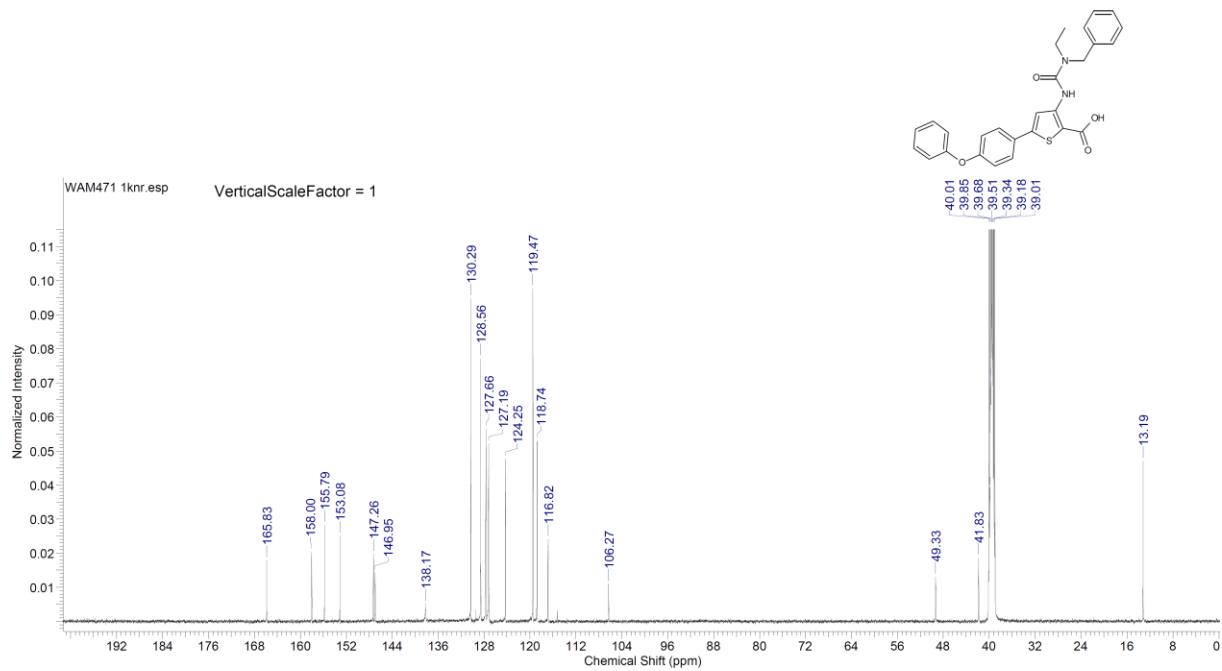
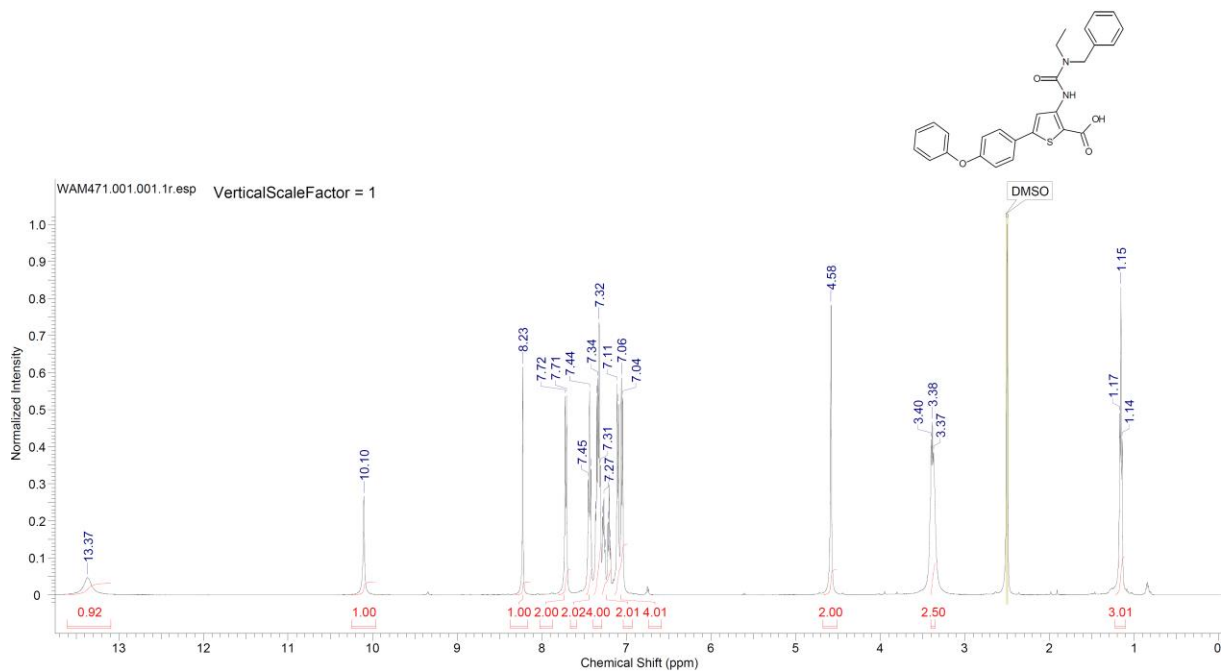
RT: 0.00 - 7.49



NL:  
3.12E6  
UV\_VIS\_1  
UV  
WAM471

WAM471 #1261-1266 RT: 5.65-5.67 AV: 6 NL: 4.73E8  
T: FTMS + p ESI Full ms [120.0000-1400.0000]





## References

- (1) Sahner, J. H., Groh, M., Negri, M., Haupenthal, J., and Hartmann, R. W. (2013) Novel small molecule inhibitors targeting the "switch region" of bacterial RNAP. Structure-based optimization of a virtual screening hit, *Eur J Med Chem* 65, 223–231. DOI: 10.1016/j.ejmech.2013.04.060.
- (2) Elgaher, W. A. M., Fruth, M., Groh, M., Haupenthal, J., and Hartmann, R. W. (2014) Expanding the scaffold for bacterial RNA polymerase inhibitors. Design, synthesis and structure–activity relationships of ureido-heterocyclic-carboxylic acids, *RSC Adv* 4, 2177–2194. DOI: 10.1039/C3RA45820B.
- (3) Elgaher, W. A. M., Sharma, K. K., Haupenthal, J., Saladini, F., Pires, M., Real, E., Mely, Y., and Hartmann, R. W. (2016) Discovery and Structure-Based Optimization of 2-Ureidothiophene-3-carboxylic Acids as Dual Bacterial RNA Polymerase and Viral Reverse Transcriptase Inhibitors, *J Med Chem* 59, 7212–7222. DOI: 10.1021/acs.jmedchem.6b00730.